

Wavenumber-dependent Gilbert damping in metallic ferromagnets

Yi Li¹ and W. E. Bailey¹

*Dept. of Applied Physics & Applied Mathematics, Columbia University,
New York NY 10027, USA*

(Dated: 28 January 2014)

New terms to the dynamical equation of magnetization motion, associated with spin transport, have been reported over the past several years. Each newly identified term is thought to possess both a real and an imaginary effective field leading to fieldlike and dampinglike torques on magnetization. Here we show that three metallic ferromagnets possess an imaginary effective-field term which mirrors the well-known real effective-field term associated with exchange in spin waves. Using perpendicular standing spin wave resonance between 2-26 GHz, we evaluate the magnitude of the finite-wavenumber (k) dependent Gilbert damping α in three typical device ferromagnets, $\text{Ni}_{79}\text{Fe}_{21}$, Co, and $\text{Co}_{40}\text{Fe}_{40}\text{B}_{20}$, and demonstrate for the first time the presence of a k^2 term as $\Delta\alpha = \Delta\alpha_0 + A_k \cdot k^2$ in all three metals. We interpret the new term as the continuum analog of spin pumping, predicted recently, and show that its magnitude, $A_k=0.07\text{-}0.1 \text{ nm}^2$, is consistent with transverse spin relaxation lengths as measured by conventional (interlayer) spin pumping.

The dynamical behavior of magnetization for ferromagnets (FM) can be described by the Landau-Lifshitz-Gilbert (LLG) equation^{1,2}:

$$\dot{\mathbf{m}} = -\mu_0|\gamma|\mathbf{m} \times \mathbf{H}_{\text{eff}} + \alpha\mathbf{m} \times \dot{\mathbf{m}} \quad (1)$$

where μ_0 is the vacuum permeability, $\mathbf{m} = \mathbf{M}/M_s$ is the reduced magnetization unit vector, \mathbf{H}_{eff} is the effective magnetic field, γ is the gyromagnetic ratio, and α is the Gilbert damping parameter. The LLG equation can be equivalently formulated, for small-angle motion, in terms of a single complex effective field term³ along the equilibrium direction, as $\tilde{H}_{eff} = H_{eff} - i\alpha\omega/|\gamma|$; damping torque is included in the imaginary part of \tilde{H}_{eff} . For all novel spin-transport related terms to the LLG identified so far⁴⁻¹⁰, each real (conservative) effective field term is mirrored by an imaginary (dissipative) counterpart. In spin-transfer torque, there exist both conventional⁴ (Slonczewski) and field-like¹¹ terms in the dynamics. In spin-orbit torques (spin Hall^{6,7} and Rashba^{8,9} effect) dampinglike and fieldlike components have been theoretically predicted¹² and most terms have been experimentally identified⁷⁻⁹. For pumped spin current¹⁰, theory predicts real and imaginary spin mixing conductances¹³ $g_r^{\uparrow\downarrow}$ and $g_i^{\uparrow\downarrow}$ which introduce imaginary and real effective fields, respectively.

It is well known that the exchange interaction, responsible for ferromagnetism, contributes a real effective field (fieldlike torque) proportional to k^2 in spin waves^{14,15}. It is then natural to ask whether a corresponding imaginary effective field term might exist, contributing a dampinglike torque to spin waves. Remarkably, this is a question which has not been addressed in prior experiments. Previous studies of ferromagnetic resonance (FMR) linewidth of spin waves¹⁶⁻²⁰ were typically operated at fixed frequency, not allowing separation of intrinsic (Gilbert) and extrinsic linewidths. Experiments have been carried out on thick FM films, susceptible to a large eddy current damping contribution²¹. Any wavenumber-dependent linewidth broadening in these systems has been attributed to eddy currents or inhomogeneous broadening, not intrinsic torques which appear in the LLG equation.

Recently Tserkovnyak *et al.*^{22,23} and Zhang *et al.*²⁴ have identified the theoretical possibility of a wavenumber-dependent Gilbert damping term for spin waves originating from local spin-current transport. The proposed damping torque is framed as a continuum analog of the (interlayer) spin pumping effect^{10,25-27}, in which antiphase precession of separated FM layers drives ("pumps") spin currents into nearby spin sink layers and the loss of angular momentum is manifested as an enhanced damping α ²⁸. In the *intralayer* spin pumping

model^{22,23}, discretized elements of a continuous FM layer, precessing out of phase as in a $k \neq 0$ spin wave, take the place of separate FM layers. The analogous Gilbert damping enhancement of the spin wave is predicted to be quadratic in the wavenumber k , as

$$\Delta\alpha_{\text{ISP}} = A_k k^2, \quad A_k = \frac{|\gamma|\sigma_{\perp}}{M_s} \quad (2)$$

where A_k is defined as the spin diffusion coefficient and the transverse spin conductivity, σ_{\perp} , is the continuum counterpart of the interfacial spin mixing conductance $g^{\uparrow\downarrow}$.

In this Manuscript, we present a study of wavenumber-dependent Gilbert damping of three different metallic ferromagnets using perpendicular standing spin wave resonance (PSSWR). PSSWR measurements at variable frequency make it possible to separate intrinsic (Gilbert) damping α of a given spin wave from extrinsic contributions to linewidth. Further advantages of PSSWR measurements for the isolation of k -dependent α include its excitation of a well-defined wavenumber k , its absence of two-magnon scattering contributions to linewidth²⁹, and sub-nm control over spin wave boundary profiles in the thickness direction. In our measurements, we have characterized the Gilbert damping α as a function of thickness (t) for the uniform mode (α_u) and the first spin wave resonance (SWR) mode (α_s). We find a k^2 -dependent increased damping $\Delta\alpha = \alpha_u - \alpha_s$ for small thicknesses, as predicted by the intralayer spin pumping theory^{22,23}. By fitting the transverse spin conductivity σ_{\perp} to the measured values of A_k , we estimate the spin relaxation length λ_{sr} to be very short, 1-2 nm, in reasonable agreement with our prior experimental estimates of the transverse spin decoherence length³⁰ from interlayer spin pumping. Our results support the existence of an imaginary effective field term for spin waves, mirroring the k^2 -dependent real effective field from exchange as predicted in Refs. 8 and 9.

Films with the structure Si/SiO₂(substrate)/Ta(5 nm)/Cu(5 nm)/FM(t)/Cu(5 nm)/Ta(5 nm) (FM = Ni₇₉Fe₂₁ (Py), Co and Co₄₀Fe₄₀B₂₀, t = 25-200 nm) were deposited by UHV magnetron sputtering with a base pressure of 5×10^{-9} Torr. The samples were characterized by field-swept, variable frequency FMR over 2-26 GHz using a coplanar waveguide with biasing field H_B applied normal to the sample surface (Fig. 1a,b). The uniform and SWR modes can be excited selectively for H_B near different resonance fields. Figure 1(c),(d) shows the lineshapes of two Py films (t = 75 nm and 200 nm). Lorentzian-derivative absorption signals are measured and fitted to extract the resonance field H_{res} and the full-width half-maximum linewidth $\Delta H_{1/2}$.

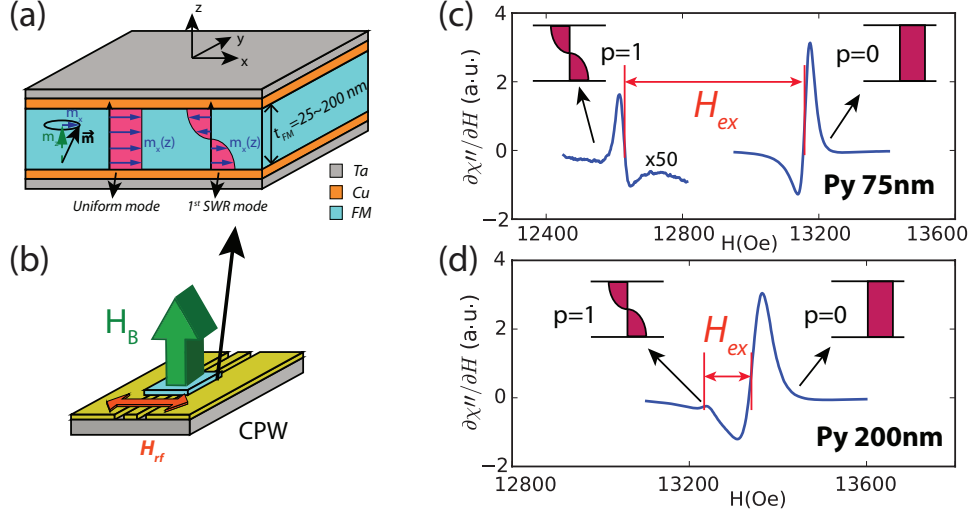


FIG. 1. (a) Layered sample structures showing the transverse component of precessing magnetization \mathbf{m} for uniform and first spin wave modes. (b) Sample configuration on coplanar waveguide (CPW) for the FMR (PSSWR) experiment. (c), (d) 10 GHz FMR spectra of the uniform mode (high field) and SWR mode (lower field) in (c) Py 75 nm and (d) 200 nm. The mode splittings H_{ex} are denoted in each case.

The resonance fields for the two modes are separated by the exchange field H_{ex} through the Kittel relation:

$$\frac{\omega}{|\gamma|} = \mu_0(H_{res} - M_{eff} + H_{ex}) \quad (3)$$

where H_{res} is the resonance field, M_{eff} is the effective magnetization and $|\gamma|/2\pi = g_{eff}/2 \cdot 27.99$ GHz/T. The exchange splitting is given by $\mu_0 H_{ex} = (2A/M_s)k^2$, where A is the exchange stiffness constant and k is the wavenumber. In a PSSWR mode, $k = p\pi/t$ where $p = 0$ for the uniform mode and $p = 1$ for the first SWR mode. The fitted $\mu_0 M_{eff}$ are 1.00, 1.47 and 1.53 T for Py, Co and CoFeB, respectively. The deviation of the $\mu_0 M_{eff}$ in Co from the bulk value³¹ 1.8 T is attributed to (0001) texture and magnetocrystalline anisotropy³².

Figure 2(a-d) shows the frequency dependence of linewidth $\Delta H_{1/2}$ of Py for $t = 25$ nm, 40 nm, 75 nm and 200 nm. For thicker films ($t = 200$ nm, Fig. 2d) the uniform mode linewidth is very large. This is due to eddy current damping^{21,33,34} which contributes an additional Gilbert-like damping term proportional to the conductivity and t^2 . The SWR mode linewidth has a much smaller eddy-current contribution^{19,20}, which we neglect in our analysis. As the film thickness decreases ($t = 75$ nm, Fig. 2c), the difference of the two slopes of $\Delta H_{1/2}$ as a function of frequency f also decreases. At $t = 40$ nm (Fig. 2b), below which

eddy current damping is negligible in the films³⁴ (see solid line, Fig. 2e), the frequency-dependent linewidths of the two modes become nearly equal. As the thickness drops further ($t = 25$ nm, Fig. 2a), the linewidths of the SWR mode surpass the values in the uniform mode, particularly for higher frequency. This effect is unrelated to eddy current damping, which is negligible at these thicknesses and has the opposite sign. Another mechanism dominates the Gilbert damping of the $p = 1$ mode when t is small.

The Gilbert damping coefficients α_u and α_s were extracted through $\Delta H_{1/2} = \Delta H_0 + 2\alpha\omega/|\gamma|$ where ΔH_0 is the inhomogeneous broadening. In the uniform modes, taking α and ΔH_0 as fitting parameters yields an average $\Delta H_0 = 3.7, 1.3$ and 2.1 Oe for Py, Co and CoFeB, respectively (Fig. 2e *inset, top*). The small inhomogeneous broadenings are consistent with negligible large-scale lateral inhomogeneities in the films. In the SWR modes, the lowest frequency attainable from Eq. (2) is close to $\gamma H_{ex}/2\pi$, proportional to $1/t^2$. For the thinnest film in Py, $t = 25$ nm, the SWR frequency range is 18-26 GHz (Fig. 2a). In this case we fix ΔH_0 from the uniform mode data. It should be noted that α_s could be overestimated by this method if a larger inhomogeneous broadening is present for the SWR, but this does not appear to be the case. An inhomogeneous broadening in SWR modes can be induced by having a small thickness variation in the films¹⁸⁻²⁰, proportional to $1/t^2 \cdot (\delta t/t)$ where δt is the thickness variation. We exclude this mechanism by plotting ΔH_0 of the SWR mode (Fig. 2e *inset, bottom*) and finding no $1/t^2$ dependence (fixed $\delta t/t$) or $1/t^3$ dependence (fixed δt). The larger variance of ΔH_0 in Co from Py and CoFeB at small thickness is due to its larger exchange splitting (Fig. 3b) and thus smaller frequency range for α_s fit than Py and CoFeB with the same thickness.

Figure 2(e-g) show α_u and α_s of Py, Co and CoFeB as a function of t . For the uniform modes α_u increases monotonically with increasing t in the thickness 25-200 nm. As expected from eddy current damping, α_u varies quadratically over t as $\alpha_u = \alpha_{u0} + \alpha_E$ where α_{u0} is the intrinsic Gilbert damping coefficient and α_E is estimated by the Lock equation³³,

$$\alpha_E = \frac{\mu_0^2 |\gamma| M_s t^2}{12\rho_c} \quad (4)$$

where ρ_c is the electrical resistivity. For Py, Co and CoFeB, the fitted $\alpha_{u0}=0.0073, 0.007$ and 0.0051 ; the extracted resistivities are $16.7, 26.4$ and $36.4 \mu\Omega\cdot\text{cm}$, respectively, in the same order of the reported values by four-point measurements³⁵⁻³⁷. We note that α_E is very small for $t_F < 75$ nm in all cases. For the SWR modes the damping α_s in Py (Fig. 2e) first

decreases with decreasing t over $150 \text{ nm} < t < 200 \text{ nm}$, then increases sharply over $25 \text{ nm} < t < 75 \text{ nm}$. A similarly strong enhancement of α_s is observed in Co (Fig. 2f). In CoFeB fluctuation of α_u makes the trend less obvious in Fig. 2(g), but it is clear in the difference $\alpha_s - \alpha_u$ (Fig. 3a). The data show that the enhanced damping exists only in the SWR mode and increases rapidly at small thicknesses.

To investigate whether an imaginary effective field (damping) term exists in parallel with the real effective field (field-like) due to exchange, we plot $\Delta\alpha_k = \alpha_s - \alpha_u + \alpha_E$ (Fig. 3a) as a function of $1/t^2$, proportional to k^2 , side-by-side with the resonance field splitting $\mu_0 H_{ex}$ (Fig. 3b). The difference $\Delta\alpha_k$ excludes the eddy current effect. A linear dependence of $\Delta\alpha_k$ on $1/t^2$ mirrors the linear dependence of $\mu_0 H_{ex}$ on $1/t^2$, both showing a k^2 dependence of effective fields (imaginary and real, respectively). CoFeB 200nm has a large errorbar due to its small exchange splitting and is excluded from the fitting of slope. The data of $\Delta\alpha_k$ are fitted to a k^2 dependent formula:

$$\Delta\alpha_k = \Delta\alpha_0 + A_k k^2 \quad (5)$$

where the slope A_k is in the unit of nm^2 and $\Delta\alpha_0$ is a constant offset. In Fig. 3(a), the fitted curves of Eq. (5) are shown in solid lines, with the fitted values of $\Delta\alpha = \alpha_s - \alpha_u$ plotted in dashed lines. A good fit of the $\Delta\alpha_k$ data points can be found to the solid lines. We show the corresponding $1/t^2$ dependence of the exchange splitting field H_{ex} (Fig. 3b), with linear fits to extract the exchange stiffness A . To compare with the intralayer spin pumping model, we calculate σ_\perp using the definition of A_k in Eq. (2). Table 1 lists all the fitting parameters in the experiments and the calculated σ_\perp . The exchange stiffnesses are close to the reported measurements^{38,39}, with Py having a slightly larger value⁴⁰. The fitted values of A_k and σ_\perp are similar in the three different ferromagnets, around $0.07\text{-}0.1 \text{ nm}^{-2}$ and $3\text{-}6 \times 10^{-25} \text{ kg}\cdot\text{m/s}$, respectively.

In a previous demonstration of a novel magneto-optical technique, Nembach *et al.*⁴¹ inferred an enhanced in-plane spin wave damping in Py nanomagnets from the damping of edge modes. Applying the above theory, they estimate $\sigma_\perp = 5.8 \times 10^{-24} \text{ kg}\cdot\text{m/s}$ in Py, about 10 times larger than our measurement by PSSWR. We plot this estimate for comparison in Fig. 3(a). Note that in Ref. 41, the (two-dimensional) mode profile was known only through numerical simulation, sensitive to edge roughness; and in-plane linewidths could include two-magnon contributions. In the PSSWR data presented here, the (one-dimensional)

mode profile is well defined, two-magnon effects are absent²⁹, and we can extract the functional term of $\alpha(k)$.

The spin relaxation time τ_{sr} and the corresponding spin relaxation length λ_{sr} are evaluated from the relation $\sigma_{\perp} = \hbar^2 n_e \tau_{sr} / 4m^*$ for the transverse spin conductivity^{22,41}, where n_e is the conduction electron density, m^* is the effective mass of electrons, and $\lambda_{sr} = v_F \tau_{sr}$ with v_F the Fermi velocity. In the calculation we use the free electron mass for m^* and $n_e = k_F^3 / 3\pi^2$ with $k_F = 1.05, 0.96$ and 1.04 \AA^{-1} for Py, Co and CoFeB^{42,43}, respectively, from the measured Fermi wave number in the majority band as an approximation. We take v_F to be 2.2×10^5 and $3.3 \times 10^5 \text{ m/s}$ for Py and Co⁴²; CoFeB is assumed to take an equal v_F to that of Co. We extract $\lambda_{sr} = 0.7 \pm 0.1 \text{ nm}$ for Py, $2.2 \pm 0.4 \text{ nm}$ for Co, and $1.8 \pm 0.3 \text{ nm}$ for CoFeB, respectively. These values are in fair agreement with the expected *transverse* spin decoherence length, with theoretically calculated scale⁴⁴ of $\lambda_J = 1 - 3 \text{ nm}$ and a measured cutoff length $\lambda_C = 1.2 \pm 0.1 \text{ nm}$ ($\lambda_C \approx \lambda_J/2$) from thickness-dependent spin-pumping measurements³⁰. The estimated λ_{sr} values in the three ferromagnets are significantly below the (longitudinal) spin diffusion lengths⁴⁵ measured from spin valve structures for these films (3.3-5.3 nm in Py⁴⁶, $59 \pm 18 \text{ nm}$ in Co⁴⁷, and 4.5 nm (4.2 K) in CoFeB⁴⁸).

The observed short length scale and small contribution to wavenumber-dependent damping is fully consistent with the proposed mechanism of transverse spin current relaxation in intralayer spin pumping²³. The transverse spin currents, proportional to magnetization gradient as $-\mathbf{m} \times \partial_i \partial_t \mathbf{m}$ (Fig. 3a *inset*), relax by losing coherence of spin-up and spin-down components and decay quickly in ferromagnetic conductors; longitudinal spin currents relax by a much slower spin-flip process. In PSSWR modes, a longitudinal spin current contribution to damping might also exist according to theory²⁴, proportional to $-\partial_t \mathbf{m} \times \partial_i \mathbf{m}$. However, comparing the longitudinal spin current to the transverse term, the former is in the order of θ^2 and the latter $\sim \theta$, where θ is the precession cone angle. In our experiment θ is less than 10^{-3} rad and the longitudinal spin current can be ignored. Thus we conclude that the k -dependent Gilbert damping enhancement is most consistent with transverse spin current relaxation.

There exists, in addition to the k^2 -dependent term, a k -independent offset between the damping of the uniform mode and the spin wave. The offset values $\Delta\alpha_0$ in Eq. (5) are negligible for Co but observable in Py and CoFeB, indicating a small reduction of the intrinsic Gilbert damping in the $p = 1$ SWR mode compared with the uniform ($p = 0$) mode.

We attribute the offset $\Delta\alpha_0$ to resistivity-like intrinsic damping⁴⁹: because $\mathbf{\hat{m}}$ is averaged through the whole film for uniform modes and has a node at the center for SWR modes (Fig. 1a), the SWR mode experiences a lower resistivity near low-resistivity Cu and thus a reduced value of α . The ordinal values of $\Delta\alpha_0$, increasing from Co (negligible) to Py to CoFeB, are consistent with this mechanism.

In summary we have experimentally identified a new term to the LLG equation, understood as an imaginary effective-field counterpart to the real effective field from exchange. We find an enhancement of Gilbert damping α proportional to k^2 in three metallic ferromagnets widely used in spin electronics. The enhancement is in reasonable quantitative agreement with the predicted intralayer spin pumping effect, consistent with transverse spin coherence lengths measured independently. The new behavior identified will be essential for optimizing the GHz response of nanoscale, confined-geometry spin electronic elements.

We acknowledge support from the National Science Foundation No. ECCS-0925829.

	$\mu_0 M_{eff}(\text{T})$	g_{eff}	$A(10^{-11}\text{J/m})$	$A_k(\text{nm}^{-2})$	$\sigma_{\perp}(10^{-25}\text{kg}\cdot\text{m/s})$	$\Delta\alpha_0$
Py	1.00	2.12	1.16 ± 0.01	0.085 ± 0.011	3.6 ± 0.5	-0.0003
Co	1.47	2.15	3.11 ± 0.06	0.076 ± 0.013	5.8 ± 1.0	0.0000
CoFeB	1.53	2.12	1.77 ± 0.02	0.099 ± 0.019	6.5 ± 1.2	-0.0010

TABLE I. Parameters fitted from the Kittel relation (Eq. 3), exchange splitting and $\Delta\alpha_k$ (Eq. 5).

REFERENCES

- ¹L. D. Landau and E. M. Lifshitz, *Phys. Z. Sowjetunion* **8**, 153 (1935).
- ²T. L. Gilbert, *Phys. Rev.* **100**, 1243 (1955).
- ³W. S. Ament and G. T. Rado, *Phys. Rev.* **97**, 1558 (1955).
- ⁴J. C. Slonczewski, *J. Magn. Magn. Mater* **159**, L1 (1996).
- ⁵L. Berger, *Phys. Rev. B* **54**, 9353 (1996).
- ⁶J. E. Hirsch, *Phys. Rev. Lett.* **83**, 1834 (1999).
- ⁷L. Liu, T. Moriyama, D. C. Ralph and R. A. Buhrman, *Phys. Rev. Lett.* **106**, 036601 (2011).

- ⁸I. M. Miron, G. Gaudin, S. Auffret, B. Rodmacq, A. Schuhl, S. Pizzini, J. Vogol and P. Gambardella, *Nature Mater.* **9**, 230 (2010).
- ⁹I. M. Miron, K. Garello, G. Gaudin, P. J. Zermatten, M. V. Costache, S. Auffret, S. Bandiera, B. Rodmacq, A. Schuhl and P. Gambardella, *Nature* **476**, 189 (2011).
- ¹⁰Y. Tserkovnyak, A. Brataas and G. E. W. Bauer, *Phys. Rev. Lett.* **88**, 117601 (2002).
- ¹¹S. Zhang, P. M. Levy and A. Fert, *Phys. Rev. Lett.* **88**, 236601 (2002).
- ¹²P. M. Haney, H. W. Lee, K. J. Lee, A. Manchon and M. D. Stiles, *Phys. Rev. B* **87**, 174411 (2013).
- ¹³M. Zwierzycki, Y. Tserkovnyak, P. J. Kelly, A. Brataas and G. E. W. Bauer, *Phys. Rev. B* **71**, 064420 (2005).
- ¹⁴C. Kittel, *Phys. Rev.* **81**, 869 (1951).
- ¹⁵J. W. Lynn, *Phys. Rev. B* **11**, 2624 (1975).
- ¹⁶C. F. Kooi, P. E. Wigen, M. R. Shanabarger and J. V. Kerrigan, *J. Appl. Phys.* **35**, 791 (1964).
- ¹⁷P. E. Wigen, *Phys. Rev.* **133**, A1557 (1964).
- ¹⁸T. G. Phillips and H. M. Rosenberg, *Phys. Lett.* **8**, 298 (1964).
- ¹⁹G. C. Bailey, *J. Appl. Phys.* **41**, 5232 (1970).
- ²⁰F. Schreiber and Z. Frait, *Phys. Rev. B* **54**, 6473 (1996).
- ²¹P. Pincus, *Phys. Rev.* **118**, 658 (1960).
- ²²E. M. Hankiewicz, G. Vignale and Y. Tserkovnyak, *Phys. Rev. B* **78**, 020404(R) (2008).
- ²³Y. Tserkovnyak, E. M. Hankiewicz and G. Vignale, *Phys. Rev. B* **79**, 094415 (2009).
- ²⁴S. Zhang and S. S. -L. Zhang, *Phys. Rev. Lett.* **102**, 086601 (2009).
- ²⁵Y. Tserkovnyak, A. Brataas, G. E. W. Bauer and B. I. Halperin *Rev. Mod. Phys.* **77**, 1375 (2005).
- ²⁶S. Mizukami, Y. Ando and T. Miyazaki, *Phys. Rev. B* **66**, 104413 (2002).
- ²⁷A. Ghosh, J. F. Sierra, S. Auffret, U. Ebels and W. E. Bailey, *Appl. Phys. Lett.* **98**, 052508 (2011).
- ²⁸B. Heinrich, Y. Tserkovnyak, G. Woltersdorf, A. Brataas, R. Urban and G. E. W. Bauer, *Phys. Rev. Lett.* **90**, 187601 (2003).
- ²⁹R. D. McMichael, M. D. Stiles, P. J. Chen and W. F. Egelhoff, Jr. *J. Appl. Phys.* **83**, 7037 (1998).
- ³⁰A. Ghosh, S. Auffret, U. Ebels and W. E. Bailey, *Phys. Rev. Lett.* **109**, 127202 (2012).

- ³¹R. C. O’Handley, *Modern Magnetic Materials Principles and Applications* p. 99, Table 3.2 (John Wiley & Sons, Inc, Canada, 2000).
- ³²R. C. O’Handley, *Modern Magnetic Materials Principles and Applications* p. 192, Table 6.1 (John Wiley & Sons, Inc, Canada, 2000).
- ³³J. Lock, *Brit. J. Appl. Phys.* **17**, 1645 (1966).
- ³⁴C. Scheck, L. Cheng and W. E. Bailey, *Appl. Phys. Lett.* **88**, 252510 (2006).
- ³⁵A. F. Mayadas, J. F. Janak and A. Gangulee, *J. Appl. Phys.* **45**, 2780 (1974).
- ³⁶S. U. Jen, Y. D. Yao, Y. T. Chen, J. M. Wu, C. C. Lee, T. L. Tsai and Y. C. Chang *J. Appl. Phys.* **99**, 053701 (2006).
- ³⁷J. W. C. de Vries, *Thin Solid Films* **167**, 25 (1988).
- ³⁸A. Conca, J. Greser, T. Sebastian, S. Klingler, B. Obry, B. Leven and B. Hillebrands, *J. Appl. Phys.* **113**, 213909 (2013).
- ³⁹X. Liu, M. M. Steiner, R. Sooryakumar, G. A. Prinz, R. F. C. Farrow and G. Harp, *Phys. Rev. B* **53**, 12166 (1996).
- ⁴⁰M. Nisenoff and R. W. Terhune, *J. Appl. Phys.* **36**, 732 (1965).
- ⁴¹H. T. Nembach, J. M. Shaw, C. T. Boone and T. J. Silva, *Phys. Rev. Lett.* **110**, 117201 (2013).
- ⁴²D. Y. Petrovykh, K. N. Altmann, H. Höchst, M. Laubscher, S. Maat, G. J. Mankey and F. J. Himpsel, *Appl. Phys. Lett.* **73**, 3459 (1998).
- ⁴³A. Useinov, O. Mryasov and J. Kosel, *J. Magn. Magn. Mater.* **324**, 2844 (2012).
- ⁴⁴J. Zhang, P. M. Levy, S. F. Zhang and V. Antropov, *Phys. Rev. Lett.* **93**, 256602 (2004).
- ⁴⁵T. Valet and A. Fert, *Phys. Rev. B* **48**, 7099 (1993).
- ⁴⁶S. Dubois, L. Piraux, J. M. George, K. Ounadjela, J. L. Duvail and A. Fert, *Phys. Rev. B* **60**, 477 (1999).
- ⁴⁷L. Piraux, S. Dubois, A. Fert and L. Belliard, *Eur. Phys. J. B* **4**, 413 (1998).
- ⁴⁸C. Ahn, K. H. Shin and W. P. Pratt, Jr., *Appl. Phys. Lett.* **92**, 102509 (2008).
- ⁴⁹K. Gilmore, Y. U. Idzerda and M. D. Stiles, *Phys. Rev. Lett.* **99**, 027204 (2007).

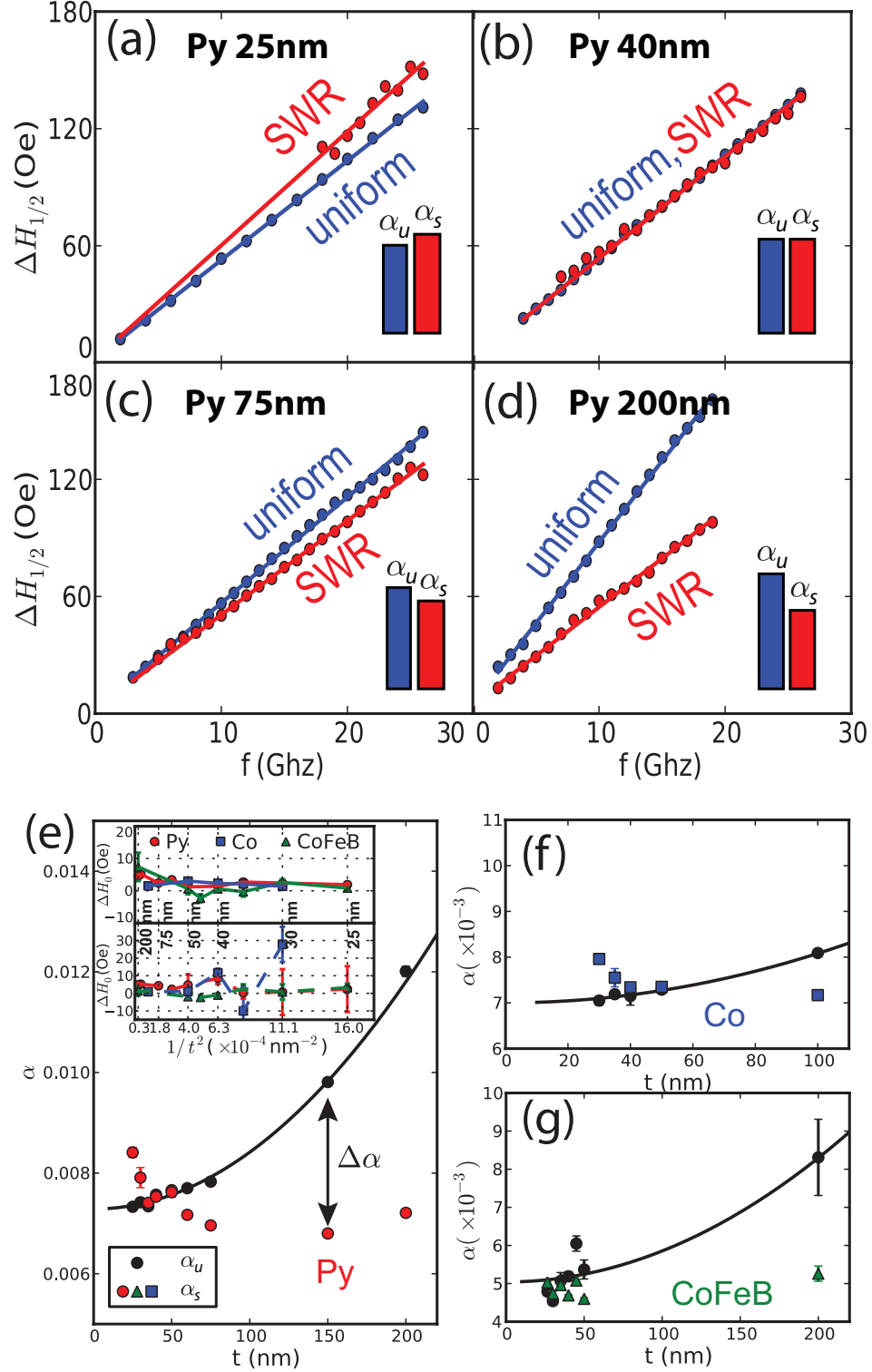


FIG. 2. (a)-(d), Half-power linewidths ($\Delta H_{1/2}$) and fittings of uniform and first SWR modes in (a) Py 25 nm, (b) 40 nm, (c) 75 nm and (d) 200 nm. (e)-(g) Thickness dependence of α_u and α_s for (e) Py, (f) Co and (g) CoFeB thin films. Solid lines are fittings to Eq. (4) plus a constant. (e) *Inset*: Inhomogeneous broadening ΔH_0 for uniform (top) and SWR (bottom) modes.

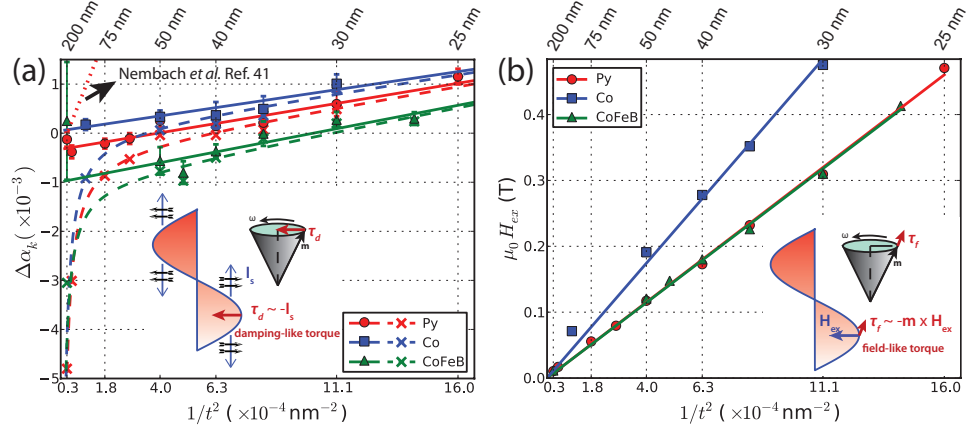


FIG. 3. (a) $\Delta\alpha_k = \alpha_s - \alpha_u + \alpha_E$ (solid) and $\Delta\alpha = \alpha_s - \alpha_u$ (cross) as a function of $1/t^2$ for Py, Co and CoFeB. (b) Exchange field H_{ex} as a function of $1/t^2$ for Py, Co and CoFeB. (a),(b) *Inset*: Illustration of (a) damping-like and (b) field-like torque in spin wave. Solid lines are fittings to (a) Eq. (5) and (b) $\mu_0 H_{ex} = (2A/M_s)k^2$. Dashed lines are fitted α_k minus α_E .